Quantum Chemical Study of Degenerate Hydride Shifts in Acyclic Tertiary Carbocations

Ivana Vinkovič Vrček,[†] Valerije Vrček,[†] and Hans-Ullrich Siehl*[,‡]

Faculty of Pharmacy and Biochemistry, University of Zagreb, 10000 Zagreb, Croatia and Department of Organic Chemistry I, University of Ulm, 89091 Ulm, Germany

Received: August 15, 2001; In Final Form: November 14, 2001

Quantum chemical calculations were carried out to study the mechanism of degenerate 1,2-, 1,3-, and 1,4-hydride shifts in acyclic tertiary carbocations 2,3-dimethyl-2-butyl, 2,4-dimethyl-2-pentyl, and 2,5-dimethyl-2-hexyl. Stable structures and transition structures were calculated at the B3LYP and MP2 levels using the 6-31G(d) and 6-311G(d,p) basis sets. The potential energy profile for these degenerate hydride shifts has global minima potential wells that correspond to the two interchanging open-chain carbocation structures and a high lying local minimum corresponding to the symmetrically hydrido-bridged intermediates. Unsymmetrically hydrido-bridged carbocations were located as transition structures. The calculated energy barriers (at the MP4/6-311G(d,p)//MP2/6-311G(d,p) level) for 1,2-, 1,3-, and 1,4-hydride shift are 3.9, 4.2, and 7.5 kcal/mol, respectively. The trend of the calculated energy barriers agrees with the experimentally observed values. Electron correlation using MP2/6-311G(d,p) is superior to B3LYP DFT hybrid methods for structures with hypercoordinated hydrogens involved in three-center two electron C−H−C bonds.

Introduction

The intermediacy of carbocations in molecular rearrangements was first suggested by Meerwein and van Emster[1] in 1922. A number of carbocations, because of their shallow potential energy surfaces, undergo fast degenerate rearrangements, leading through intramolecular hydride shifts to the related identical structures.[2] 1,2-hydride shifts in carbocations are quite common, and many carbocations are also prone to undergo fast degenerate hydride shifts to distant carbons (Scheme 1).[3] The study of the mechanism of carbocation rearrangements has led to a deeper understanding of many fundamental chemical and biochemical problems ranging from the theory of chemical structure (valence theory) to the theory of chemical reactivity and chemical activation and the biogenetic formation of terpenes and steroids. The facile hydride shift reactions of carbocations are intimately coupled with internal charge stabilization by increasing the coordination through bridging forming three-center two-electron (3c-2e) C−H−C bonds. Such hydrido-bridged carbocations can be transition structures and/or stable intermediates in hydride shift rearrangements, and sometimes these types of hypercoordinated carbocations are found to be lower in energy than their nonbridged isomers.

The solvolysis studies of Prelog et al.[4] and Cope et al.[5] have shown that medium-sized cycloalkyl rings undergo direct transannular hydride shifts via transition structures which resemble μ-hydrido-bridged carbocation structures. The first μ-hydrido-bridged carbocation, the cyclooctyl cation, prepared in solution and characterized by NMR spectroscopy was reported in 1978.[6] During the past two decades, a variety of other cyclic hydrido-bridged carbocations have been reported.[7] In acyclic carbocations such as **I** ⇆ **I′** where *n* is 0, 1, or 2 (Scheme 1) degenerate 1,2-, 1,3-, and 1,4-hydride shifts[8] as well as higher order hydride shifts[9] have been investigated experimentally using NMR spectroscopic methods. A fast rearrangement process eventually allows us to observe kinetic line broadening and equilibrium isotope effects (EIE).[10] Typical barriers for such hydride shifts obtained from dynamic NMR spectroscopy in solution range from 3 to 12 kcal/mol. The observation of a barrier implies a dynamic process such as an equilibrium between carbocation structures **I** and **I′** where the symmetric μ-hydrido-bridged structure **II** is higher in energy than the interchanging open chain structures.

SCHEME 1

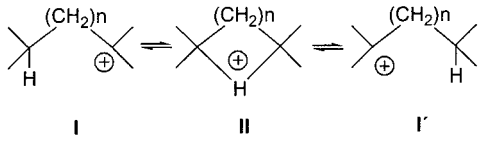

Details of the mechanism of hydride shift rearrangements such as whether hydrido-bridged structures of type **II** are high lying intermediates or transition structures are not easily accessible by experimental dynamic NMR spectroscopy. Therefore, we have performed a model study of acyclic tertiary carbocations undergoing 1,2-, 1,3-, and 1,4-hydride shifts using high level quantum chemical calculations, based on DFT-hybrid (B3LYP)[11] and Møller−Plesset second-order perturbation (MP2(FC))[12] theory, to establish the structures of energy minima and transition structures for these carbocations in some more detail.

Computational Methods

The quantum chemical calculations were performed using the Gaussian 98 program suite (revision A.9) on SUN enterprise servers and SGI Origin and SuSE LINUX PC's.[13] All structures were fully optimized (in the specified symmetry) using the DFT-hybrid and Møller−Plesset perturbation theory. The B3LYP functional was used, which combines Becke's three-parameter exchange functional with the correlation functional of Lee, Yang, and Parr.[14] The ab initio calculations were performed using frozen core (FC) second-order MP2 perturbation correction

* To whom correspondence should be addressed. E-mail: ullrich.siehl@chemie.uni-ulm.de. Fax: +49-(0)731 50 22787.
[†] Faculty of Pharmacy and Biochemistry, University of Zagreb.
[‡] Department of Organic Chemistry I, University of Ulm.

10.1021/jp013158u CCC: $22.00
Published on Web 02/05/2002

SCHEME 2

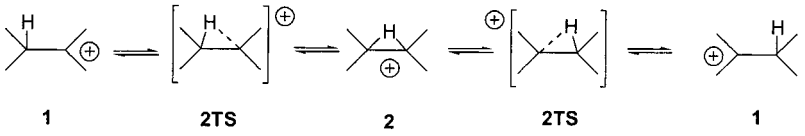

TABLE 1: Total Energies and Relative Energy Differences for Structures 1, 2, and 2TS

level of theory	cation	*E* (Hartree)	ZPE (Hartree)	ΔE (kcal/mol)[a]	NImag (v, cm^{-1})
B3LYP/6-31G(d)	**1**	−236.188522	0.175503	0	0
	2	−236.176442	0.173203	7.58 (6.12)	1 (−450)
B3LYP/6-311G(d,p)	**1**	−236.250794	0.173763	0	0
	2	−236.240314	0.171420	6.58 (5.11)	1 (−438)
MP2/6-31G(d)	**1**	−235.282151	0.179134	0	0
	2	−235.272818	0.177588	5.86 (4.89)	0
	2TS	−235.272767	0.177102	5.89 (4.61)	1 (−225)
MP2/6-311G(d,p)	**1**	−235.457522	0.176384	0	0
	2	−235.450591	0.175051	4.35 (3.50)	0
	2TS	−235.450460	0.174564	4.43 (3.29)	1 (−219)
MP4/6-311G(d,p)//	**1**	−235.568250	0.176384	0	
MP2/6-311G(d,p)[b]	**2**	−235.560466	0.175051	4.88 (4.04)	
	2TS	−235.560364	0.174564	4.96 (3.92)	

[a] Relative energy difference values including ZPE (not scaled) corrections are given in parentheses. [b] ZPE correction values calculated at the MP2/6-311G(d,p) level of theory.

and fourth-order MP4(SDTQ) theory with single, double, triple, and quadruple substitutions.[15]

The standard split valence and polarized 6-31G(d) basis set was employed in the geometry optimizations and frequency calculations. For comparison, we also carried out calculations with the larger basis set 6-311G(d,p). A vibrational analysis was performed at the same level of theory (except for MP4 calculations) in order to determine the zero-point vibrational energy (ZPE) and to characterize each stationary point as a minimum (NImag = 0) or transition structure (NImag = 1). The optimized MP2/6-311G(d,p) geometries were subjected to single-point energy calculations at MP4 level; thus, our final level is MP4(SDTQ)/6-311G(d,p)//MP2/6-311G(d,p). Corrections for ZPE (not scaled) are included in the calculated energies. The relative energies are given in kcal/mol with respect to the most stable corresponding isomer and are listed in Tables 1, 3, and 5.

Results and Discussion

1,2-Hydride Shift. 2,3-dimethyl-2-butyl cation (**1**) is an equilibrating carbocation (Scheme 2) that undergoes a rapid degenerate 1,2-hydride shift.[16] Kates and Saunders[17] measured the rate of degenerate 1,2-hydride shift. The free energy of activation ($\Delta G^{\#} = 3.1$ kcal/mol at −138 °C) was determined from line broadening in ^{13}C NMR spectra.

At the B3LYP/6-31G(d) level, we have located the minimum structure **1** (NImag = 0) and a symmetrical (C_2 point group) hydrido-bridged structure **2** which, at this level of theory, was found to be a transition structure (NImag = 1) for a degenerate 1,2-hydride shift. Total energies and geometrical parameters for the structures are presented in Tables 1 and 2, respectively.

Minimum structure **1** is the β-C−C-hyperconjugative isomer in which the C_2-C_3 bond is involved in hyperconjugative stabilization of the positive charge (Figure 1). This bond is elongated (1.596 Å) in comparison to the C_2-C_4 (1.532 Å) bond. The angle $C_1C_2C_3$ of the bond involved in hyperconjugation is reduced to 101.5° as compared to the bond angle $C_1C_2C_4$ (117.8°). No β-C−H-hyperconjugative isomers were located on the corresponding energy surface. During the optimization at the B3LYP/6-31G(d) level, their geometries converged to the more stable C−C-hyperconjugative isomers.

TABLE 2: Selected Geometrical Parameters for Structures 1, 2, and 2TS

cation	geometrical parameter[a]	B3LYP/ 6-31G(d)	B3LYP/ 6-311G(d,p)	MP2/ 6-31G(d)	MP2/ 6-311G(d,p)
1	$d(C_1C_2)$	1.463	1.461	1.447	1.445
	$d(C_2C_3)$	1.596	1.595	1.593	1.601
	$d(C_2C_4)$	1.532	1.530	1.523	1.524
	$\angle(C_1C_2C_3)$	101.5	101.6	98.3	96.5
	$\angle(C_1C_2C_4)$	117.8	117.8	118.5	118.8
2	$d(C_1H)$	1.327	1.329	1.314	1.317
	$d(C_2H)$	1.327	1.329	1.314	1.317
	$d(C_1C_2)$	1.421	1.419	1.413	1.416
	$\angle(C_1C_2C_3)$	122.4	122.4	122.2	122.1
	$\angle(C_1HC_2)$	64.7	64.5	65.0	65.1
2TS	$d(C_1H)$			1.413	1.463
	$d(C_2H)$			1.245	1.227
	$d(C_1C_2)$			1.415	1.421
	$\angle(C_1C_2C_3)$			122.1	121.6
	$\angle(C_1HC_2)$			63.9	63.1

[a] Bond lengths are in angstroms, and bond angles are in degrees.

The hydrido-bridged structure **2** is characterized by symmetrical C_1-H-C_2 bridging in which the C−H bonds are elongated (1.327 Å) and the bond angle C_1HC_2 is 64.7° (Figure 1). The imaginary frequency which corresponds to the symmetry breaking C−H−C (↔) vibrational mode is 450i cm^{-1}.

The calculated energy barrier for the degenerate 1,2-hydride shift at the B3LYP/6-31G(d) level (including ZPE correction) is 6.1 kcal/mol (Table 1) which is not in an agreement with the experimental finding ($\Delta G^{\#} = 3.1$ kcal/mol).

When extra valence functions and polarization functions are added in the basis set (B3LYP/6-311G(d,p) level) for the optimization of **1** and **2**, no significant change neither in geometries nor in relative energy differences were found (see Tables 1 and 2). The total energies and geometry parameters for the B3LYP/6-311G(d,p) optimized structures are presented in Tables 1 and 2, respectively.

At the MP2/6-31G(d) level of theory, the geometries and relative energies for **1** and **2** differ somewhat from those obtained at the B3LYP level (see Tables 1 and 2). The hyperconjugative interaction between the C_2C_3 bond and the 2p orbital at the formal carbenium ion center in **1** is favored by

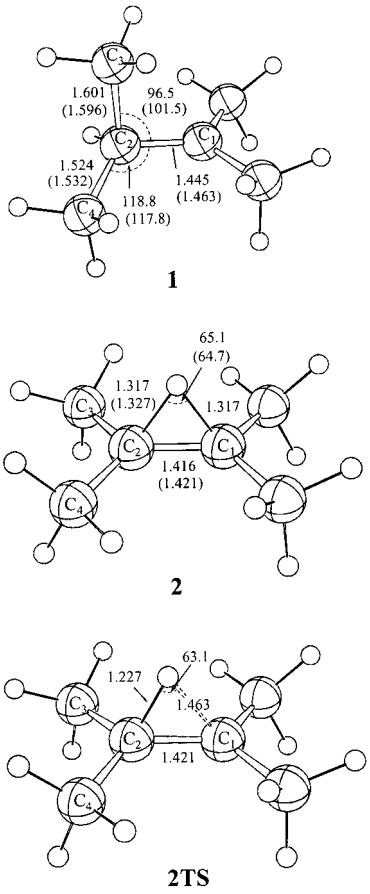

Figure 1. Optimized structures of **1**, **2**, and **2TS** at the MP2/6-311G-(d,p) level of theory (the B3LYP/6-31G(d) level in parentheses). Bond lengths are in angstroms, and angles are in degrees.

the MP2 method as indicated by the 3° smaller $C_1C_2C_3$ bond angle for **1** and shorter bridging CH bonds (1.314 Å) in the C_2 symmetry structure of **2** (Table 2).

At the MP2/6-31G(d) level, both structures **1** and **2** were found to be minima (NImag = 0). This reflects the flat energy surface in the transition structure region and also indicates that the B3LYP method is probably not appropriate to correctly describe the hydrido-bridged structure **2**. At the HF/6-31G(d) level of theory, the hydrido-bridged structure **2** was also found to be a transition structure (NImag = 1), but Schleyer et al. interpreted this as an artifact at the noncorrelated HF level.[18] Similarly, it was found for the C_2 and C_s symmetric hydrido-bridged structures of the 2-butyl cation to have one imaginary frequency at the HF/6-31G(d) level, but subsequent characterization at the MP2/6-31G(d) and MP2/6-31G(d,p) levels showed that these structures are indeed minima.[19]

At the MP2/6-311G(d,p) level of theory, both carbocation structures **1** and **2** are also minima. Cation **1** was found to be 4.4 kcal/mol (3.5 kcal/mol when ZPE is included) more stable than the symmetrical (C_2) hydrido-bridged cation **2**. These results suggest that the potential energy surface for the 1,2-hydride shift has three minima, two degenerate trivalent carbocations **1** and a high-lying intermediate, hydrido-bridged carbocation **2**. Similarly, for the 2-butyl cation, it has been proposed that the best fit with the experimental data could be obtained by a model assuming both the hydrido-bridged structure and two degenerate open chain carbocations to be present in a fast equilibrium.[20,21]

The transition structure **2TS** connecting **1** and **2** was located at the MP2/6-31G(d) and MP2/6-311G(d,p) levels. The only

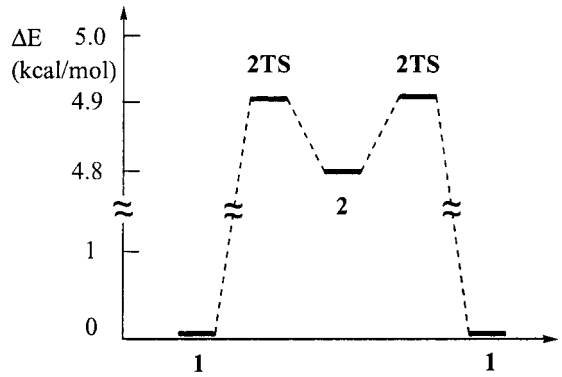

Figure 2. Reaction profile for 1,2-hydride shift rearrangement in the 2,3-dimethyl-2-butyl cation (**1**) calculated at the MP4/6-311G(d,p)// MP2/6-311G(d,p) level of theory.

imaginary vibrational mode (219*i* cm^{-1} at the MP2/6-311G-(d,p) level) is associated with the movement of the bridging hydrogen atom between the two carbon atoms. Although the hydrido-bridged structure **2** (NImag = 0) has C_2 symmetry, the transition structure **2TS** (NImag = 1) has no symmetry. An unsymmetrical three-center two-electron C−H−C bond characterizes this structure (Figure 1). At the MP2/6-311G(d,p) level, the C_2−H bond length is 1.227 Å and the C_1−H distance is 1.463 Å (Figure 1). The corresponding bridging angle C_1HC_2 is 63°, i.e., 2° smaller than the one in the geometry of **2**. At the same level of theory, the transition structure **2TS** is only 0.1 kcal/mol less stable than **2** if the zero-point vibrational energy is not included (Table 1). If the ZPE is taken into account, the transition structure **2TS** becomes more stable than **2**, indicating that the potential energy surface in this region is very flat. An unusual inversion of the stationary points, an intermediate and a transition structure, with very small energy difference in a flat transition structure region of the potential energy surface, when vibrational energy contributions are included, has been reported.[22] It is known that in such cases the harmonic approximation is no longer valid and leads to an incorrect picture.[23]

A more complete treatment of electron correlation was made by performing MP4(SDTQ)/6-311G(d,p) single-point energy calculations for the MP2/6-311G(d,p) optimized structures (Table 1). According to these results, the potential energy profile (Figure 2) for the 1,2-hydride shift has three potential-wells that correspond to two equivalent carbocation structures **1** and a symmetrical hydrido-bridged high-lying intermediate **2** and two maxima which correspond to the unsymmetrically bridged transition structure **2TS**.

1,3-Hydride Shift. The 2,4-dimethyl-2-pentyl cation (**3**) undergoes a degenerate 1,3-hydride shift.[24] A line-shape analysis, assuming the 1,3-hydride shift, yields an activation energy of 8.5 kcal/mol. There are two alternative mechanisms possible (Scheme 3). In the pathway **3** ⇆ **6TS** ⇆ **5** ⇆ **6TS** ⇆ **3**, **3** undergoes successive 1,2-hydride shifts via the secondary carbocation intermediate **5**. The other pathway **3** ⇆ **7** ⇆ **8TS** ⇆ **7** ⇆ **3** involves a corner protonated cyclopropane structure **7**. The pathway **3** ⇆ **6TS** ⇆ **5** ⇆ **6TS** ⇆ **3** is not consistent with the observed spectral changes, whereas the mechanism in which the intermediacy of protonated cyclopropane is assumed is highly unlikely on the basis of energy estimates.[25]

High-level quantum chemical calculations were performed for the species **3**−**8TS** involved in these three possible reaction paths. No stationary points were found for the corner-protonated cyclopropane intermediate (**7**) and the edge-protonated transition structure (**8TS**). During the geometry optimizations at the

SCHEME 3

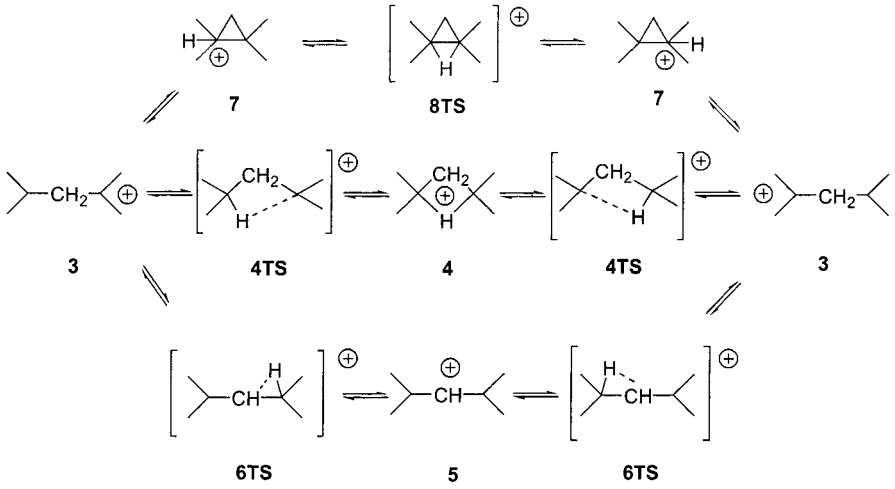

TABLE 3: Total Energies and Relative Energy Differences for Structures 3a, 3b, 3c, 4, 4TS, 5, and 6TS

level of theory	cation	*E* (Hartree)	ZPE (Hartree)	ΔE (kcal/mol)[a]	NImag (ν, cm^{-1})
B3LYP/6-31G(d)	**3a**	−275.504325	0.204017	0	0
	3b	−275.501154	0.202900	1.99 (1.29)	0
	3c	−275.503125	0.204210	0.75 (0.87)	0
	4	−275.486239	0.203500	11.35 (11.03)	1 (−480)
	5	−275.488774	0.204860	9.76 (10.29)	0
	6TS	−275.484789	0.202666	12.26 (11.41)	1 (−309)
B3LYP/6-311G(d,p)	**3a**	−275.577088	0.201966	0	0
	3b	−275.574542	0.201003	1.50 (1.54)	0
	3c	−275.575923	0.202198	0.73 (0.88)	0
	4	−275.560015	0.201597	10.71 (10.48)	1 (−452)
	5	−275.560819	0.202799	10.21 (10.73)	0
	6TS	−275.558534	0.200917	11.64 (10.98)	1 (−152)
MP2/6-31G(d)	**3a**	−274.450089	0.208572	0.73 (0.27)	0
	3c	−274.451245	0.209304	0	0
	4	−274.442417	0.208496	5.54 (5.03)	1 (−155)
	5	−274.438899	0.209644	7.75 (7.96)	0
	6TS	−274.431840	0.207328	12.18 (10.96)	1 (−218)
MP2/6-311G(d,p)	**3a**	−274.654995	0.205497	1.09 (0.71)	0
	3c	−274.656732	0.206269	0	0
	4	−274.651288	0.205629	3.41 (3.01)	0
	4TS	−274.651287	0.205511	3.42 (3.00)	1 (−72)
	5	−274.644772	0.206334	7.51 (7.55)	0
	6TS	−274.638185	0.204534	11.64 (10.55)	1 (−148)
MP4/6-311G(d,p)// MP2/6-311G(d,p)[b]	**3a**	−274.783499	0.205497	0.46 (0.04)	
	3c	−274.784240	0.206269	0	
	4	−274.776878	0.205511	4.62 (4.14)	
	4TS	−274.776862	0.205629	4.63 (4.23)	
	5	−274.770514	0.206334	8.61 (8.65)	
	6TS	−274.766417	0.204534	11.18 (10.10)	

[a] Relative energy difference values including ZPE (not scaled) corrections are given in parentheses. [b] ZPE correction values calculated at the MP2/6-311G(d,p) level of theory.

B3LYP and MP2 levels of theory, the geometries of **7** and **8TS** converged to the more stable minimum structures **3** and **4**, respectively. For the 1-propyl cation, however,[26] which is the parent analogue of the 2,4-dimethyl-2-pentyl cation, structures of type **7** or **8TS** were located as stationary points. These ab initio calculations were done at the 4-31G//STO-3G level of theory and indicated that the 1,3-hydride shift in the 1-propyl cation might proceed via an edge-protonated transition structure with an activation energy of approximately 10 kcal/mol. Our theoretical study of the rearrangements **3** ⇆ **4** ⇆ **3** and **3** ⇆ **5** ⇆ **3** (Scheme 3) reveals new intermediates **3a**, **3b**, and **3c** and transition structure **4TS** and **6TS** not previously characterized Both the experimental and quantum chemical results are in agreement that the rearrangement of **3** is a direct degenerate 1,3-hydride shift between two tertiary carbon centers.

At the B3LYP/6-31G(d) level, both the β-C−C- and β-C−H-hyperconjugative isomers of the open-chain cation **3** are found as minima at the corresponding potential energy surface (Figure 3). At this level of theory, the C−C-hyperconjugative isomer **3a** is found to be 1.3 kcal/mol (including ZPE correction) more stable than the C−H-hyperconjugative isomer **3b** (Table 3). The hyperconjugative interaction between the C_2C_3 bond and the formally empty 2p orbital at the C_1 carbon atom in the isomer **3a** can be deduced from the relative lengthening of the C_2C_3 bond to 1.627 Å and from the $C_1C_2C_3$ bond angle value of 109.2 °. The C_2−H hydrogen bond involved in the hyperconjugative

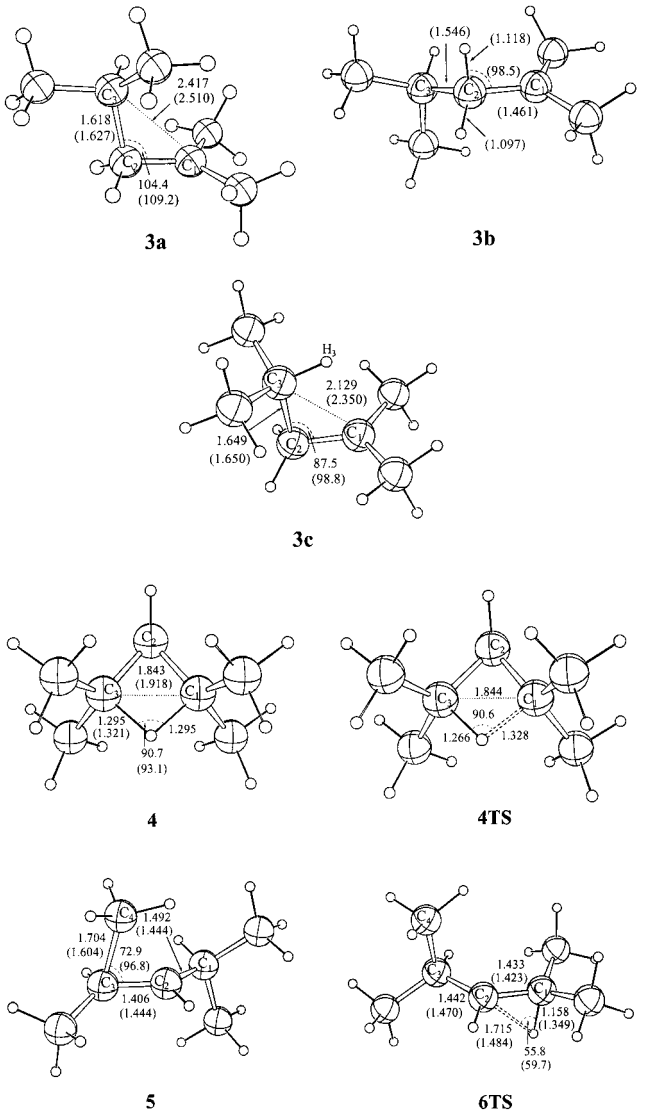

Figure 3. Optimized structures of **3a**, **3c**, **4**, **4TS**, **5**, and **6TS** at the MP2/6-311G(d,p) level of theory (the B3LYP/6-31G(d) level in parentheses). CH-hyperconjugative isomer **3b** was located only at the B3LYP/6-31G(d) level. Bond lengths are in angstroms, and angles are in degrees.

interaction in the isomer **3b** shows an extended bond length of 1.118 Å and a small C_1C_2H bond angle of 99.4 °.

At the B3LYP/6-31G(d) level of theory, we have located another stable structure for cation **3** in which β-C−C-hyperconjugation occurs. This isomer **3c** has an eclipsed conformation of the C_2-H and C_1-C_2 bonds and is 0.9 kcal/mol (including ZPE correction) less stable than the corresponding C−C-hyperconjugative isomer **3a** which has a staggered conformation along the C_2C_3 bond. These two isomers **3a** and **3c** can be related to the geometries of methyl-staggered and methyl-eclipsed 1-propyl cation.[27] The eclipsed isomer **3c** has C_s symmetry, and the geometric parameters are substantially different from the staggered isomer **3a**. Thus, the $C_1C_2C_3$ bond angle is smaller (98.9 vs. 109.2°) and the C_2C_3 bond is elongated (1.650 vs. 1.627 Å) resulting in a closer approach to a bridged arrangement. In the isomer **3c**, the carbon atom C_3 is closer to the carbocationic center than in **3a** (2.350 vs 2.510 Å, respectively). This is an optimal geometry for a direct 1,3-shift of the hydrogen atom H_3. This isomer **3c** could be alternatively regarded as a distorted corner-protonated cyclopropane. At the B3LYP/6-31G(d) level of theory, the structure **4** was found to be a transition structure connecting two identical isomers **3c**. It is a symmetrical (C_2 point group) hydrido-bridged structure characterized by elongated C_1-H and C_3-H bonds (1.321 Å) and a C_1-C_3 distance of 1.918 Å, whereas the corresponding bridging C_1HC_3 angle is 93.1° (Figure 3). The geometry of this four-membered ring is planar, and the only imaginary vibration frequency ($480i$ cm^{-1}) is associated to the symmetrical movement of the bridged hydrogen atom either to C_1 or to the C_3 carbon atom, which is consistent with the degenerate 1,3-hydride shift.

TABLE 4: Selected Geometrical Parameters for Structures 3a, 3b, 3c, 4, 4TS, 5, and 6TS

cation	geometrical parameter[a]	B3LYP/ 6-31G(d)	B3LYP/ 6-311G(d,p)	MP2/ 6-31G(d)	MP2/ 6-311G(d,p)
3a	$d(C_2C_3)$	1.627	1.624	1.613	1.618
	$d(C_1C_2)$	1.449	1.447	1.439	1.439
	$d(C_1C_3)$	2.510	2.510	2.434	2.417
	$\angle(C_1C_2C_3)$	109.2	109.5	105.6	104.4
3b	$d(C_1C_2)$	1.465	1.461		
	$d(C_2C_3)$	1.552	1.546		
	$d(C_2H)$	1.118	1.118		
	$\angle(C_1C_2C_3)$	120.5	121.0		
	$\angle(C_1C_2H)$	99.35	98.5		
3c	$d(C_1C_2)$	1.441	1.438	1.422	1.422
	$d(C_2C_3)$	1.650	1.649	1.645	1.649
	$d(C_1H_3)$	2.282	2.283	2.094	2.037
	$d(C_1C_3)$	2.350	2.353	2.175	2.129
	$\angle(C_1C_2C_3)$	98.8	99.1	90.1	87.5
4	$d(C_1H)$	1.321	1.320	1.296	1.295
	$d(C_3H)$	1.321	1.320	1.296	1.295
	$d(C_1C_3)$	1.918	1.915	1.845	1.843
	$\angle(C_1HC_3)$	93.1	92.9	90.7	90.7
4TS	$d(C_1H)$				1.328
	$d(C_3H)$				1.266
	$d(C_1C_3)$				1.844
	$\angle(C_1HC_3)$				90.6
5	$d(C_1C_2)$	1.444	1.441	1.434	1.492
	$d(C_2C_3)$	1.444	1.441	1.434	1.406
	$d(C_3C_4)$	1.604	1.604	1.597	1.704
	$\angle(C_2C_3C_4)$	96.8	96.9	94.1	72.9
6TS	$d(C_1C_2)$	1.423	1.425	1.425	1.433
	$d(C_1H)$	1.484	1.638	1.679	1.715
	$d(C_2H)$	1.349	1.181	1.167	1.158
	$d(C_2C_3)$	1.470	1.462	1.449	1.442
	$\angle(C_1HC_2)$	59.7	58.0	56.7	55.8

[a] Bond lengths are in angstroms and bond angles are in degrees.

At the B3LYP/6-31G(d) level, we have also located a transition structure **6TS** which connects the β-C−H-hyperconjugative isomer **3b** and the secondary carbocation **5** (Figure 3). The structure **6TS** represents the transition structure ($152i$ cm^{-1}) for the alternative mechanism of successive 1,2-hydride shifts (Scheme 3). At this level of theory, the unsymmetrically bridged structure **6TS** was found to be 12.3 kcal/mol less stable than the global minimum structure **3a** (Table 3). These results indicate that the successive 1,2-shift rearrangement in the 2,4-dimethyl-2-pentyl cation **3** is energetically less favorable (E_a= 12.3 kcal/mol) than the direct 1,3-hydride shift (E_a= 11.4 kcal/mol).

Introduction of extra valence and polarization functions in the basis set (B3LYP/6−311(d,p) level of theory) had no significant effects neither on the calculated geometries of **3**−**8TS** cations (Table 4) nor on the relative energies (Table 3).

However, somewhat different results were obtained at the MP2/6-31G(d) level of theory. At this level, the β-C−H-hyperconjugative isomer **3b** does not exist at the potential energy surface and its geometry on optimization collapsed to the β-C−

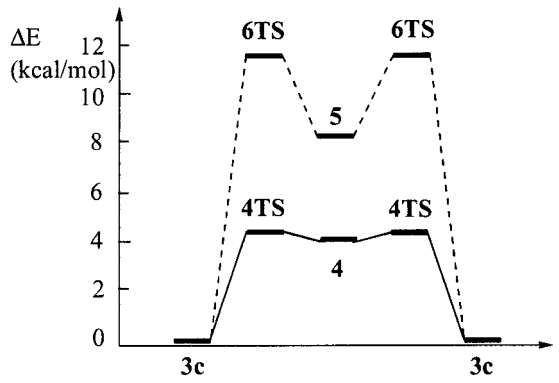

Figure 4. Reaction profiles for 1,3-hydride shift (thick line) and the successive 1,2-hydride shift (dotted line) rearrangement in 2,4-dimethyl-2-pentyl cation (**3**) calculated at the MP4/6-311G(d,p)//MP2/6-311G(d,p) level of theory.

C-hyperconjugative form **3a**. In contrast to the B3LYP results, the most stable structure at the potential energy surface was found to be the eclipsed β-C−C-hyperconjugative isomer **3c**. It is 0.3 kcal/mol more stable than the staggered β-C−C-hyperconjugative isomer **3a** and 5 kcal/mol more stable than the symmetrical hydrido-bridged structure **4** (Table 3). This gives an energy barrier (including ZPE correction) of only 5 kcal/mol for the degenerate 1,3-hydride shift rearrangement.

The corresponding energy barriers (including ZPE correction) calculated at the B3LYP levels are considerably higher (11 and 10.5 kcal/mol at the B3LYP/6-31G(d) and B3LYP/6-311G(d,p) level, respectively) indicating that electron correlation effects considered by the MP2 method favor the bridged structures to a great extent.[28] The bridging C_1HC_3 bond angle value for the structure **4** calculated at the MP2/6-31G(d) level is smaller (90.7°), the C_1C_2 (1.845 Å) and C_1H (1.290 Å) distances are shorter. Similar effects were found for the unsymmetrically bridged transition structure **6TS** (see Table 3).

At the MP2/6-311G(d,p) level of theory, the eclipsed β-C−C-hyperconjugative isomer **3c** has the lowest energy (Table 3). It is 1.1 kcal/mol more stable than the staggered β-C−C-hyperconjugative isomer **3a** and 3.4 kcal/mol more stable than the symmetrically bridged structure **4**. In contrast to the MP2/6-31G(d) and DFT-hybrid results, at the MP2/6-311G(d,p) level of theory, the symmetrical structure **4** was found to be a minimum (NImag = 0). The transition structure **4TS**, which connects symmetrical structures **4** (C_2 point group) and **3c** (C_s point group) was located only at this level of theory. The energy and geometrical parameters of the structure **4TS** are similar to that of **4** (Tables 3 and 4). However, the partially bridged **4TS** has no symmetry. Its imaginary frequency (72*i* cm^{-1}) is associated to the movement of the bridging hydrogen atom between C_1 and C_3. The insignificant energy difference between **4** and **4TS** (10 cal/mol) and the small value of the lowest vibrational frequency in **4** (52 cm^{-1}) indicates that potential energy surface for the 1,3-shift process is extremely flat. In such cases, geometry optimizations and frequency calculations at a higher level of theory, which include larger basis set, are necessary to correctly describe the potential energy surface for hydride shift rearrangements. The results demonstrate that the 6-311G(d,p) basis set with an extra valence functions and p functions added to hydrogens is important for adequate descriptions of systems with hypercoordinated hydrogens involved in three-center two electron C−H−C bond.

Finally, MP4(SDTQ)/6-311G(d,p) single-point energy calculations for the MP2/6-311G(d,p) optimized structures were performed to account for a more complete treatment of electron correlation. The calculated energy barrier (Table 3) for the direct 1,3-hydride shift is 4.6 kcal/mol, whereas the corresponding energy barrier for the successive 1,2-hydride shift is 11.2 kcal/mol (Figure 4). These results show some discrepancies from the experimental value (8.5 kcal/mol) obtained in solution. However, the results indicate clearly that the symmetrical 1,3-hydride shift is energetically more favorable than successive 1,2-hydride shift. This corroborates the experimental findings.

1,4-Hydride Shift. For the 2,5-dimethyl-2-hexyl cation (**9**), Brouwer and van Doorn observed no line broadening in the ^1H NMR spectrum up to −50 °C.[29] However, Saunders and Stofko using spin-transfer saturation techniques proved that 1,4-hydride shifts do occur in cation **9**. The energy barrier for this rearrangement was estimated from this experiments to be equal to 12−13 kcal/mol which is even higher than the experimental barrier for the 1,3-hydride shift in the 2,4-dimethyl-2-pentyl cation (**3**).

In contrast to the 2,3-dimethyl-2-butyl cation (**1**) and 2,4-dimethyl-2-pentyl cation (**3**), this system gives similar results for both the DFT-hybrid and MP2 methods in terms of relative energies and geometrical parameters. At all levels employed (Table 5), three stationary points **9**, **10**, and **10TS** were located on the potential energy surface (Scheme 4). The open-chain structure **9** is the global minimum, and the symmetrically bridged (C_2 point group) structure **10** is a high-lying intermediate (Figure 5). At the MP2/6-311G(d,p) level, this five-membered ring structure **10** is 4.6 kcal/mol less stable (including ZPE correction) than the open-chain cation **9**. The transition structure

TABLE 5: Total Energies and Relative Energy Differences for Structures 9, 10, and 10TS

level of theory	cation	*E* (Hartree)	ZPE (Hartree)	Δ*E* (kcal/mol)[a]	NImag (ν, cm^{-1})
B3LYP/6-31G(d)	**9**	−314.819723	0.232811	0	0
	10	−314.802955	0.231386	10.52 (9.63)	0
	10TS	−314.802866	0.231223	10.58 (9.59)	1 (−167)
B3LYP/6-311G(d,p)	**9**	−314.902940	0.230478	0	0
	10	−314.886781	0.229212	10.14 (9.35)	0
	10TS	−314.886651	0.229186	10.22 (9.41)	1 (−175)
MP2/6-31G(d)	**9**	−313.618363	0.238342	0	0
	10	−313.606509	0.237840	7.44 (7.12)	0
	10TS	−313.603762	0.236688	9.16 (8.12)	1 (−318)
MP2/6-311G(d,p)	**9**	−313.852925	0.234767	0	0
	10	−313.845358	0.234497	4.75 (4.58)	0
	10TS	−313.840737	0.233191	7.65 (6.66)	1 (−296)
MP4/6-311G(d,p)// MP2/6-311G(d,p)[b]	**9**	−313.998330	0.234767	0	–
	10	−313.989389	0.234497	5.61 (5.44)	–
	10TS	−313.984784	0.233191	8.50 (7.51)	–

[a] Relative energy difference values including ZPE (not scaled) corrections are given in parentheses. [b] ZPE correction values calculated at the MP2/6-311G(d,p) level of theory.

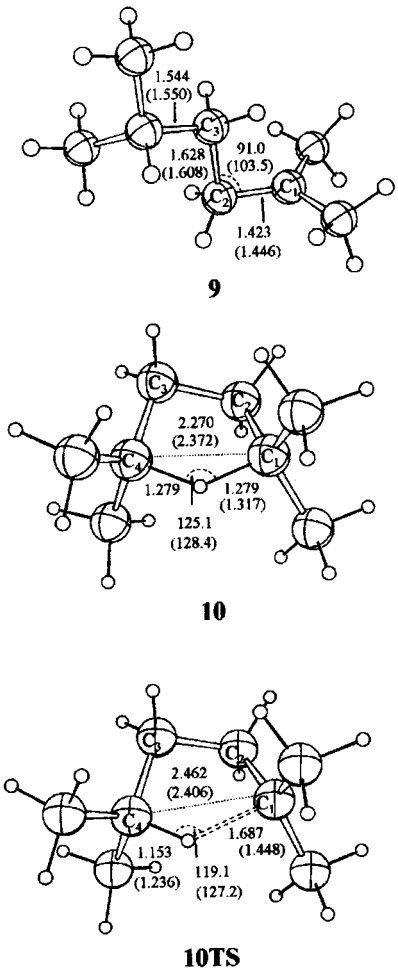

Figure 5. Optimized structures of **9**, **10**, and **10TS** at the MP2/6-311G(d,p) level of theory (the B3LYP/6-31G(d) level in parentheses). Bond lengths are in angstroms, and angles are in degrees.

SCHEME 4

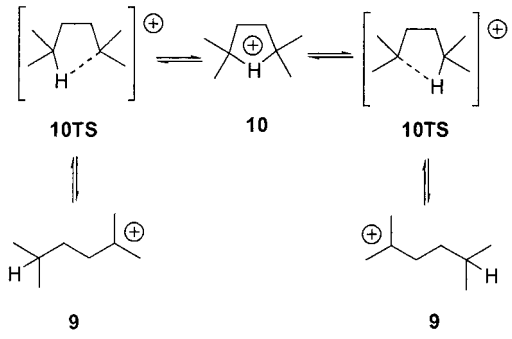

10TS is characterized by unsymmetrical C_1HC_4 bridging (Figure 5). It is 7.7 kcal/mol less stable than the global minimum structure **9**. Thus, the energy barrier, calculated at the MP2/6-311G(d,p) level, for the 1,4-hydride shift in the 2,5-dimethyl-2-hexyl cation (**9**) in the gas phase is 7.7 kcal/mol.

The MP2/6-311G(d,p) optimized geometries of **9**, **10**, and **10TS** are presented in Figure 5. The calculated bond lengths and bond angles in the carbocation **9** are similar at all levels (Table 6) except that the MP2 geometries show larger hyperconjugatively induced distortions. The C_2C_3 bond in **9** that eclipses the formally empty 2p orbital at the C_1 carbon is lengthened to 1.628 Å, and the bond angle $C_1C_2C_3$ is reduced to 91°. The five-membered ring hydrido-bridged carbocation structure **10** has an envelope conformation where $C_4-H-C_1-C_2$ are in the same plane (Figure 5). The CH bonds involved in bridging are elongated to 1.279 Å, the bond angle C_1HC_4 is 125.1°, and the distance between C_1 and C_4 is 2.270 Å at the MP2/6-311G(d,p) level (Table 6).

TABLE 6: Selected Geometrical Parameters for Structures 9, 10, and 10TS

cation	geometrical parameter[a]	B3LYP/ 6-31G(d)	B3LYP/ 6-311G(d,p)	MP2/ 6-31G(d)	MP2/ 6-311G(d,p)
9	$d(C_1C_2)$	1.446	1.445	1.426	1.423
	$d(C_2C_3)$	1.608	1.605	1.617	1.628
	$d(C_3C_4)$	1.550	1.548	1.542	1.544
	$\angle(C_1C_2C_3)$	103.5	103.8	93.6	91.0
	$\angle(C_2C_3C_4)$	110.5	110.7	108.8	108.5
10	$d(C_1C_4)$	2.372	2.371	2.289	2.270
	$d(C_1H)$	1.317	1.316	1.285	1.279
	$d(C_4H)$	1.317	1.316	1.285	1.279
	$\angle(C_1C_2C_3)$	102.9	102.9	101.3	100.8
	$\angle p(C_1HC_4)$	128.4	128.5	125.9	125.1
10TS	$d(C_1C_4)$	2.406	2.407	2.697	2.462
	$d(C_1H)$	1.448	1.473	1.618	1.687
	$d(C_4H)$	1.236	1.220	1.167	1.153
	$\angle(C_1C_2C_3)$	103.6	103.6	109.5	103.4
	$\angle(C_1HC_4)$	127.2	126.5	117.2	119.1

[a] Bond lengths are in angstroms, and bond angles are in degrees.

The energies (Table 5) and geometrical parameters (Table 6) of the transition structure **10TS** are similar to that of **10** but lacking the C_2 axis of symmetry. The bridging in **10TS** is unsymmetrical: the distance between C_1 and the bridging hydrogen is 1.687 Å, and the length of the C_4-H bond is 1.153 Å (at the MP2/6-311G(d,p) level). The imaginary frequency mode (296*i* cm^{-1} at the MP2/6-311G(d,p) level) of **10TS** corresponds to the movement of the bridging hydrogen atom between the C_1 and C_4 carbon atoms. Alternative mechanisms to the 1,4-hydride shift in **9** have been ruled out experimentally. The calculated energy barrier of 7.5 kcal/mol is in a reasonable agreement with the barrier of 12−13 kcal/mol estimated in SbF_5/SO_2ClF solution.

Concluding Remarks

The degenerate hydride shifts in acyclic tertiary carbocations have been investigated computationally by means of DFT-hybrid and Møller−Plesset perturbation theory methods. It has been shown that the B3LYP level of theory is not appropriate to correctly describe these systems. Electron correlation such as the MP2 method and basis sets such as 6-311G(d,p) are required for systems with hypercoordinated hydrogens involved in three-center two electron C−H−C bonds. A comparative study of 1,2-, 1,3-, and 1,4-hydride shifts reveals the similar potential energy profiles for these processes. Two global minima that correspond to two equivalent open-chain carbocation structures, one local minimum that corresponds to a symmetrical hydrido-bridged high-lying intermediate, and two maxima that correspond to two unsymmetrically bridged transition structures have been located at the corresponding potential energy surfaces. The energy barrier values calculated at the MP4/6-311G(d,p)//MP2/6-311G(d,p) level of theory increase with the size of the ring formed in the hydrido-bridged transition structures. The calculated energy barriers for 1,2-, 1,3-, and 1,4-hydride shift at the MP4/6-311G(d,p)//MP2/6-311G(d,p) level including ZPE (not scaled, MP2/6-311G(d,p)) are 3.9, 4.2, and 7.5 kcal/mol, respectively, which is in line with experimental observations.

Acknowledgment. We gratefully acknowledge financial support by the Deutsche Forschungsgemeinschaft (DFG) and

the Fonds der Chemischen Industrie. We also acknowledge support for V.V. by the Alexander von Humboldt Foundation. We thank Thomas Nau, Computer Center, University of Ulm, for adaption of the Gaussian program suite.

Supporting Information Available: *xyz* coordinates for structures **1**−**10**TS. This information is available free of charge via the Internet at http://pubs.acs.org.

References and Notes

(1) Meerwein, H.; van Emster, K. *Ber. Deuts. Chem. Ges.* **1922**, *55*, 2500.

(2) (a) Olah, G. A.; Prakash, G. K. S.; Sommer, J. *Superacids*; Wiley-Interscience: New York, 1985; Vol. 3, p 128. (b) Saunders, M.; Chandrasekhar, J.; Schleyer, P. v. R. In *Rearrangements in Ground and Excited States*; deMayo, P., Ed.; Academic Press: New York, 1980; Vol. 1, p 1.

(3) (a) Ahlberg, P.; Jonsall, G.; Engdahl, C. *Adv. Phys. Org. Chem.* **1983**, 223 and references therein. (b) Siehl, H.-U.; Walter, H. *J. Chem. Soc., Chem. Comm.* **1985**, 76.

(4) Prelog, V.; Traynham, J. G. In *Molecular Rearrangements*; deMayo, P., Ed.; Interscience: New York, 1963; Vol. 1, p 593.

(5) Cope, A. C.; Martin, M. M.; McKervey, M. A. *Quart. Rev.* **1966**, *20*, 119.

(6) Kirchen, R. P.; Sorensen, T. S.; Wagstaff, K. E. *J. Am. Chem. Soc.* **1978**, *100*, 6761.

(7) (a) McMurry, J. E.; Lectka, T. *J. Am. Chem. Soc.* **1993**, *115*, 10167. (b) Sorensen, T. S.; Whitworth, S. M. *J. Am. Chem. Soc.* **1990**, *112*, 8135. (c) McMurry, J. E.; Lectka, T. *J. Am. Chem. Soc.* **1990**, *112*, 869. (d) McMurry, J. E.; Lectka, T. Hodge, C. N. *J. Am. Chem. Soc.* **1989**, *112*, 8867. (e) Kirchen, R. P.; Sorensen, T. S.; Wagstaff, K.; Walker, A. M. *Tetrahedron* **1986**, *42*, 1063. (f) McMurry, J. E.; Hodge, C. N. *J. Am. Chem. Soc.* **1984**, *106*, 6450. (g) Kirchen, R. P.; Okazawa, N.; Ranganayakulu, K.; Rauk, A.; Sorensen, T. S. *J. Am. Chem. Soc.* **1981**, *103*, 597. (h) Galasso, V. *Chem. Phys.* **1999**, *241*, 247. (i) Galasso, V. *Int. J. Quantum Chem.* **1998**, *70*, 313.

(8) Saunders, M.; Stofko, J. J. *J. Am. Chem. Soc.* **1973**, *95*, 252.

(9) (a) Walter, H. Ph.D. Thesis, University of Tuebingen, 1984. (b) Roever A.; Siehl, H.-U. *Abstracts 9th IUPAC Conference on Physical Organic Chemistry*, P89; Regensburg, Germany, 1988. (c) Lenoir, D.; Siehl, H.-U. In *Houben-Weyl Methoden der Organischen Chemie*; Hanack, M., Ed.; Thieme: Sttutgart, Germany, 1990; Vol. E19c, p 36. (d) Sun, F.; Sorensen, T. S. *J. Am. Chem. Soc.* **1993**, *115*, 77.

(10) (a) Siehl, H.-U. *Adv. Phys. Org. Chem.* **1987**, *23*, 63.

(11) (a) Becke, A. D. *J. Chem. Phys.* **1993**, *98*, 5648. (b) Stevens, P. J.; Devlin, F. J.; Chablowski, C. F.; Frisch, M. J. *J. Chem. Phys.* **1994**, *98*, 11623.

(12) (a) Møller, C.; Plesset, M. S. *Phys. Rev.* **1934**, *46*, 618. (b) Frisch, M. J.; Head-Gordon, M.; Pople, J. A. *Chem. Phys. Lett.* **1990**, *66*, 281. (b) Trucks, G. W.; Frisch, M. J.; Andres, J. L.; Schlegel, H. B. *J. Chem. Phys.* **1995**.

(13) Frisch, M. J.; Trucks, G. W.; Schlegel, H. B.; Scuseria, G. E.; Robb, M. A.; Cheeseman, J. R.; Zakrzewski, V. G.; Montgomery, J. A., Jr.; Stratmann, R. E.; Burant, J. C.; Dapprich, S.; Millam, J. M.; Daniels, A. D.; Kudin, K. N.; Strain, M. C.; Farkas, O.; Tomasi, J.; Barone, V.; Cossi, M.; Cammi, R.; Mennucci, B.; Pomelli, C.; Adamo, C.; Clifford, S.; Ochterski, J.; Petersson, G. A.; Ayala, P. Y.; Cui, Q.; Morokuma, K.; Malick, D. K.; Rabuck, A. D.; Raghavachari, K.; Foresman, J. B.; Cioslowski, J.; Ortiz, J. V.; Stefanov, B. B.; Liu, G.; Liashenko, A.; Piskorz, P.; Komaromi, I.; Gomperts, R.; Martin, R. L.; Fox, D. J.; Keith, T.; Al-Laham, M. A.; Peng, C. Y.; Nanayakkara, A.; Gonzalez, C.; Challacombe, M.; Gill, P. M. W.; Johnson, B. G.; Chen, W.; Wong, M. W.; Andres, J. L.; Head-Gordon, M.; Replogle, E. S.; Pople, J. A. *Gaussian 98*, revision A.9; Gaussian, Inc.: Pittsburgh, PA, 1998.

(14) Lee, C.; Yang, W.; Parr, R. G. *Phys. Rev B* **1988**, *37*, 785.

(15) Krishnan, R.; Frisch, M. J.; Pople, J. A. *J. Chem. Phys.* **1980**, *72*, 4244.

(16) Olah, G. A.; Lukas, J. *J. Am. Chem. Soc.* **1967**, *89*, 2227, 4731.

(17) Saunders, M.; Kates, M. R. *J. Am. Chem. Soc.* **1978**, *100*, 7082.

(18) Buzek, P.; Schleyer, P. von R.; Sieber, S.; Koch, W.; Carneiro, J. W. de M.; Vancik, H.; Sunko, D. E. *J. Chem. Soc., Chem. Commun.* **1991**, 671.

(19) Sieber, S.; Buzek, P.; Scleyer, P. v. R.; Koch, W.; Carneiro, J. W. de M. *J. Am. Chem. Soc.* **1993**, *115*, 259.

(20) Olah, G. A.; Donovan, D. J. *J. Am. Chem. Soc.* **1977**, *99*, 5026.

(21) (a) Walker, G. Ph.D. Thesis, Yale University. (b) Saunders, M.; Walker, G. Unpublished results (private communication).

(22) Lee, I.; Kim, C. K.; Li, H. G.; Lee, B.-S.; Lee, H. W. *Chem. Phys. Lett.* **2000**, *320*, 307.

(23) Schreiner, P. R.; Schleyer, P. v. R.; Schaefer, H. F. *J. Org. Chem.* **1997**, *62*, 4216.

(24) Brouwer, D. M.; van Doorn, J. A. *Recl. Trav. Chim. Pays-Bas.* **1969**, *88*, 573.

(25) Saunders, M.; Vogel, P.; Hagen, L. L.; Rosenfeld, J. *Acc. Chem. Res.* **1973**, *6*, 53.

(26) (a) Radom, L.; Pople, J. A.; Buss, V.; Schleyer, P. v. R. *J. Am. Chem. Soc.* **1972**, *94*, 311. (b) Radom, L.; Pople, J. A.; Buss, V.; Schleyer, P. v. R. *J. Am. Chem. Soc.* **1971**, *93*, 1813.

(27) (a) Farcasiu, D.; Hancu, D. *J. Am. Chem. Soc.* **1999**, *121*, 7173.

(28) (a) Schleyer, P. v. R.; Maerker, C. *Pure Appl. Chem.* **1995**, *67*, 755. (b) Schleyer, P. v. R.; Maerker, C.; Buzek, P.; Sieber, S. Accurate Carbocation Structure: Verification of Computed Geometries by NMR, IR, and X-ray Diffraction. In *Stable Carbocations*; Prakash, G. K. S., Schleyer, P. v. R., Eds.; Wiley: New York, 1997.

(29) Brouwer, D. M.; van Doorn, J. A. *Recl. Trav. Chim. Pays-Bas.* **1970**, *89*, 333.